RESEARCH ARTICLE • OPEN ACCESS

Effect of Toxicant on One Prey and Two Competing Predators with Beddington-DeAngelis Functional Response

Kavita Makwana, Raveendra Babu A., and B.P.S. Jadon

Volume 6, Issue 1, Pages 44–59, March 2025

Received 20 February 2025, Revised 27 March 2025, Accepted 28 March 2025, Published Online 31 March 2025

To Cite this Article : K. Makwana *et al.*,"Effect of Toxicant on One Prey and Two Competing Predators with Beddington-DeAngelis Functional Response", *Jambura J. Biomath*, vol. 6, no. 1, pp. 44–59, 2025, *https://doi.org/10.37905/jjbm.v6i1.30686*

JOURNAL INFO • JAMBURA JOURNAL OF BIOMATHEMATICS

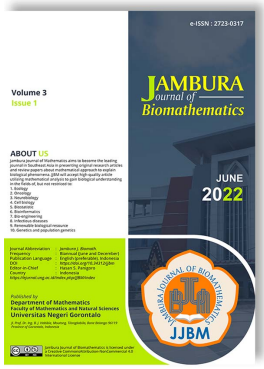

Homepage	:	http://ejurnal.ung.ac.id/index.php/JJBM/index
Journal Abbreviation	:	Jambura J. Biomath.
Frequency	:	Biannual (June and December)
Publication Language	:	English
DOI	:	https://doi.org/10.37905/jjbm
Online ISSN	:	2723-0317
Editor-in-Chief	:	Hasan S. Panigoro
Publisher	:	Department of Mathematics, Universitas Negeri Gorontalo
Country	:	Indonesia
OAI Address	:	http://ejurnal.ung.ac.id/index.php/jjbm/oai
Google Scholar ID	:	XzYgeKQAAAAJ
Email	:	editorial.jjbm@ung.ac.id

JAMBURA JOURNAL • FIND OUR OTHER JOURNALS

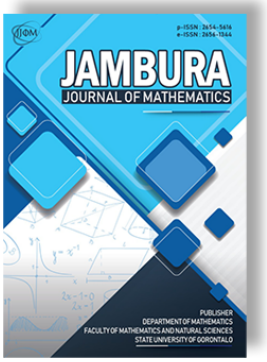

Jambura Journal of Mathematics

Jambura Journal of Mathematics Education

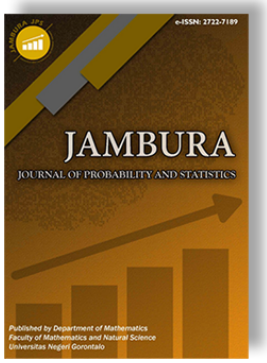

Jambura Journal of Probability and Statistics

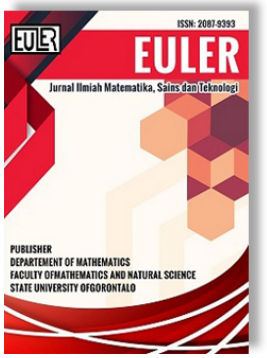

EULER : Jurnal Ilmiah Matematika, Sains, dan Teknologi

Jambura Journal of Biomathematics, Volume 6, Issue 1, Pages 44–59, March 2025 https://doi.org/10.37905/jjbm.v6i1.30686

Research Article

Check for updates

Effect of Toxicant on One Prey and Two Competing Predators with Beddington-DeAngelis Functional Response

Kavita Makwana[1,*], **Raveendra Babu A.**[2], **and B.P.S. Jadon**[3]

[1,3]*Department of Mathematics, S.M.S. Govt. Model Science College, Gwalior 474009, India*
[2]*Department of Information & technology, Prestige Institute of Management and Research, Gwalior 474020, India*

ARTICLE HISTORY
Received 20 February 2025
Revised 27 March 2025
Accepted 28 March 2025
Published 31 March 2025

KEYWORDS
Mathematical modelling
Stability analysis
Bifurcation
Sensitivity analysis
Parameter variation

ABSTRACT. *This study investigates the dynamical behaviour of a prey-predator system with two competing predators, incorporating the Beddington–DeAngelis functional response and the effects of environmental toxicants. Analytical analysis ensures the boundedness of solutions, guaranteeing biologically feasible population dynamics. Equilibrium points are identified, and their stability is examined using local and global stability analyses. Numerical simulations validate the analytical findings, demonstrating that as the competition coefficient b_1 increases, the system transitions from a stable equilibrium to periodic oscillations and eventually to chaotic behaviour. Furthermore, the impact of the toxicant uptake rate d_1 is explored to assess its role in system stability. The results indicate that low levels of toxicant absorption promote oscillatory dynamics, while higher values of d_1 suppress population growth and restore stability. This highlights the dual role of toxicants in ecological systems, where moderate exposure disrupts equilibrium, but excessive accumulation can lead to stabilization. Bifurcation diagrams and time-series simulations further reinforce these transitions, revealing critical thresholds where stability is lost or regained. The study provides valuable insights into the complex interplay between toxicant dynamics, predator-prey interactions, and bifurcation phenomena. The findings emphasize the ecological implications of toxicant exposure and interspecies competition, offering potential applications in environmental management and conservation strategies.*

1. Introduction

Understanding the dynamics of predator-prey interactions is a fundamental topic in ecological modelling, with extensive studies incorporating various functional responses, delays, environmental effects, and stochastic influences [1]. One widely studied functional response in this domain is the Beddington–DeAngelis type, which effectively describes predator-prey interactions by considering mutual interference among predators. Several studies have explored its impact on ecological systems, revealing diverse dynamical behaviours ranging from stability to chaos.

Zhang et al. [2] investigated the influence of the fear effect and prey refuge in a fractional-order predator-prey system with the Beddington–DeAngelis functional response. Their study employed fractional calculus to analyse chaotic behaviour and stability. Similarly, Shao and Kong [3] extended this framework by incorporating multiple delays in deterministic and stochastic environments, providing insights into the role of time-dependent interactions in predator-prey models. Meng and Wang [4] examined a delayed diffusive model with the Beddington–DeAngelis response, focusing on bifurcation and stability properties.

Further modifications to classical models have also been explored. Rahmi et al. [5] introduced a modified Leslie–Gower model integrating the Beddington–DeAngelis functional response along with the double Allee effect and memory influence, highlighting how these factors contribute to ecosystem stability. Yu and Chen [6] analysed a competitive system with Beddington–DeAngelis interactions, revealing its complex dynamical behaviors through bifurcation analysis.

Multi-species predator-prey interactions have also been extensively studied. Babu and Gayathri [7] examined a system involving one prey and two competing predators, incorporating distributed delay to analyse stability and bifurcations. Majeed and Naji [8] explored the effects of prey refuge and the Beddington–DeAngelis response in a two-predator, one-prey system, employing bifurcation analysis and numerical simulations. Zhou and Chen [9] extended these findings to a discrete amensalism system, incorporating the Allee effect for unaffected species and demonstrating its impact on stability.

The role of environmental factors such as fear, toxicity, and fluctuations has also been a key area of research [10, 11]. Das et al. [12] analysed predator-prey interactions under the influence of fear, toxicity, and environmental carry over effects, using dynamical system modelling and bifurcation analysis. Liu et al. [13] studied a fractional-order predator-prey model incorporating toxic effects, examining bifurcation and stability properties. Misra and Babu [14–16] also studied on predator prey model with toxicant and distributed delay.

Stochastic modelling approaches have provided additional perspectives on ecological dynamics. Danane et al. [17] de-

*Corresponding Author.

Email : *kavitamakwana16@yahoo.com* (K. Makwana)
Homepage : http://ejurnal.ung.ac.id/index.php/JJBM/index / E-ISSN : 2723-0317

veloped a three-species stochastic prey-predator model driven by Levy jumps, combining Holling-II and Beddington–DeAngelis functional responses. Their findings emphasized the significance of stochastic influences on predator-prey interactions.

Additionally, bifurcation theory has been widely applied to study dynamical transitions in ecological systems. Bosi and Desmarchelier [18] provided a theoretical characterization of local bifurcations in three and four-dimensional systems, extending their applications to economic and ecological models. Wang et al. [19] conducted a bifurcation analysis of predator-prey models, detailing critical transitions in system behaviour. Kaur et al. [20] focused on chaos control in plankton dynamics by considering additional food availability, seasonality, and time delays, offering insights into the mitigation of chaotic oscillations in ecological models.

Recent advancements in fractional calculus have significantly enhanced the modeling of ecological systems, particularly in capturing complex interactions such as toxicant effects, prey refuge, and predator-prey dynamics. Fractional-order models provide a more accurate representation of memory effects and non-local interactions, making them valuable for ecological modelling [21]. According to Bhatter et al. [22], a modified Atangana-Baleanu fractional derivative was applied to model human liver function, demonstrating the effectiveness of fractional calculus in biological systems. This approach highlights the potential benefits of fractional-order derivatives in ecological models, where non-integer dynamics can better describe long-term species interactions and environmental perturbations. Similarly, Kumawat et al. [23] developed a fractional-order model for age-based COVID-19 transmission, employing Chebyshev polynomials and stability analysis to examine disease spread. Their use of fractional derivatives in epidemiological modeling aligns with the need for more precise representations of predator-prey interactions under environmental stress. Meena et al. [24] further explored fractional-order modelling by investigating tuberculosis transmission using the Caputo fractional derivative and generalized Euler's method, showcasing how fractional-order models improve the understanding of disease dynamics and control strategies. These studies collectively reinforce the importance of fractional calculus in ecological research, providing a strong foundation for extending classical predator-prey models. In this study, we incorporate fractional derivatives into a predator-prey-toxicant model to analyse the effects of toxic stress on species stability and bifurcation structures.

By incorporating toxicant effects, two competing predator species [25], and a modified Beddington–DeAngelis functional response, this study expands on previous predator-prey models. Misra and Babu [16] studied the role of toxicants in a prey-predator system, whereas Babu and Gayathri [7] studied predator competition with distributed delays. This research, however, did not completely take into consideration how inter specific competition, environmental contamination, and toxicant accumulation all affect system stability. By incorporating toxicant dynamics from the prey population and the surrounding environment, our model builds upon previous frameworks and takes into consideration indirect detrimental effects on higher trophic levels. This study aims to extend existing models by incorporating toxicant effects and exploring their influence on stability and bifurcation structures. We provide analytical and numerical results that reveal new dynamical behaviours in predator-prey interactions under toxic stress, contributing to both theoretical ecology and applied bio-mathematics.

2. Model construction

2.1. Mathematical model

We consider a three-species predator-prey system incorporating the effects of toxicants in both the environment and organisms. The functional response of the predators follows the Beddington-DeAngelis type, which accounts for both mutual interference among predators and prey-dependent predation rates. The system consists of one prey population (N) and two predator populations (P_1) and (P_2), where toxicants influence both organismal health and environmental conditions. This model builds on the structure of [7], which analyzed a similar predator-prey system, and extends the approach of [16] by incorporating the toxicant effects on multiple predator species and the environment.

The state variables and parameters:

The prey population N follows a logistic growth pattern, regulated by the intrinsic growth rate a_0 and the carrying capacity limitation b_0. However, exposure to toxicants reduces the prey's intrinsic growth rate, which is accounted for by the parameter c_0. The two predator species P_1 and P_2 rely on the prey for sustenance. The predation rates of P_1 and P_2 on the prey are given by a_1 and a_2, respectively. The efficiency with which the consumed prey biomass is converted into predator growth is represented by b_1 for P_1 and c_1 for P_2. The natural mortality rates of the two predator species are denoted by b_2 and c_2, respectively. Additionally, the presence of mutual interference among predators affects their predation efficiency, modelled by the terms $\alpha_1 P_2$ and $\alpha_2 P_1$, which represent the extent of interference from competing predators. The environmental toxicant concentration, denoted by E, changes due to an external input rate q_0, as well as natural washout at a rate e_3. Toxicants are also transferred to the prey population through uptake from the environment at a rate d_1. The concentration of toxicants within organisms, represented by O, accumulates due to prey exposure to environmental toxicants. The rate of toxicant elimination from organisms due to metabolic processes is given by e_1, while the removal of toxicants due to prey mortality occurs at a rate e_2. The dynamics of the system are governed by the following set of differential equations:

$$\begin{aligned}
\frac{dN}{dT} &= a_0 N - b_0 N^2 - \frac{a_1 N P_1}{1+N+\alpha_1 P_2} - \frac{a_2 N P_2}{1+N+\alpha_2 P_1} \\
&\quad - c_0 N O, \\
\frac{dP_1}{dT} &= \frac{b_1 a_1 N P_1}{1+N+\alpha_1 P_2} - b_2 P_1, \\
\frac{dP_2}{dT} &= \frac{c_1 a_2 N P_2}{1+N+\alpha_2 P_1} - c_2 P_2, \\
\frac{dO}{dT} &= d_1 N E - e_1 O - e_2 N O, \\
\frac{dE}{dT} &= q_0 - e_3 E - d_1 N E + e_2 N O,
\end{aligned} \tag{1}$$

with the initial conditions:

$$N(0) > 0,\ P_1(0) > 0,\ P_2(0) > 0,\ O(0) = 0,\ E(0) \geq 0.$$

2.2. Incorporation of the Beddington-DeAngelis functional response

The predation terms in the prey equation and predator equations follow the Beddington-DeAngelis functional response, which modifies the traditional Holling Type-II response by incorporating mutual interference among predators. This is represented as:

$$\frac{a_1 N P_1}{1 + N + \alpha_1 P_2}, \frac{a_2 N P_2}{1 + N + \alpha_2 P_1},$$

where, the denominator $1 + N + \alpha_1 P_2$ and $1 + N + \alpha_2 P_1$ represent the effects of both prey density and predator interference on predation efficiency. α_1 and α_2 capture the mutual interference effect, reducing predation efficiency as predator density increases.

2.3. Biological interpretation of the model

The formulated system of differential equations represents the interactions between prey, two predator species, and the toxicant in both organisms and the environment. Each equation corresponds to a biological process that governs species survival and toxicant accumulation.

1. **Prey Population** N: The term $-b_0 N^2$ represents the logistic growth of the prey, where higher prey density leads to stronger competition for resources, reducing the growth rate. This ensures that the prey population does not grow indefinitely and stabilizes at a carrying capacity. However, exposure to toxicants affects its survival, modeled by the toxicant-dependent mortality term $c_0 NO$. Predation by the two predator species follows the Beddington-DeAngelis functional response, incorporating both prey availability and predator interference.
2. **Predator Populations** P_1, P_2: The two predator species consume prey at the rates of a_1 and a_2, converting consumed biomass into their own growth with efficiencies b_1 (for P_1) and c_1 (for P_2). Each predator faces natural mortality, given by $b_2 P_1$ and $c_2 P_2$. The presence of mutual interference $\alpha_1 and \alpha_2$ reduces the predation efficiency when predator densities are high.
3. **Toxicant in Organisms** O **and Environment** E: The environmental toxicant E accumulate from external sources q_0 and degrade at a rate $e_3 E$. Prey absorb toxicants through environmental exposure $d_1 NE$, and these accumulate internally within organism. Toxicant elimination occurs through metabolic processes $e_1 O$ and prey mortality $e_2 NO$. These factors together determine toxicant persistence in the ecosystem.

This biological interpretation strengthens the connection between the mathematical framework and real-world ecological conditions, emphasizing how toxicant interactions influence species survival and the system stability.

2.4. Non-dimensionalization of the model

To simplify the system, we introduce the following dimensionless variables:

$$\begin{aligned}
N &= \frac{a_0 x}{b_0}, & P_1 &= \frac{y}{\alpha_2}, & P_2 &= \frac{z}{\alpha_1}, & T &= \frac{t}{a_0},\\
E &= \frac{a_0 c_e}{d_1}, & O &= \frac{a_0 c_p}{e_2}, & a &= \frac{a_0}{b_0}, & g &= \frac{c_0}{e_2},\\
b &= \frac{a_1}{a_0 \alpha_2}, & c &= \frac{a_2}{a_0 \alpha_1}, & p &= \frac{b_1 a_1}{b_0}, & q &= \frac{b_2}{a_0},\\
r &= \frac{c_1 a_2}{b_0}, & s &= \frac{c_2}{a_0}, & p_0 &= \frac{e_2}{b_0}, & p_1 &= \frac{e_1}{a_0},\\
t_1 &= \frac{d_1 q_0}{a_0^2}, & t_2 &= \frac{e_3}{a_0}, & t_3 &= \frac{d_1}{b_0}.
\end{aligned}$$

Using these transformations, the rescaled non-dimensionalized system is given by:

$$\frac{dx}{dt} = x(1-x) - gxc_p - \frac{bxy}{1 + ax + z} - \frac{cxz}{1 + ax + y} \tag{2}$$

$$\frac{dy}{dt} = \frac{pxy}{1 + ax + z} - qy \tag{3}$$

$$\frac{dz}{dt} = \frac{rxz}{1 + ax + y} - sz \tag{4}$$

$$\frac{dc_p}{dt} = p_0 x c_e - p_1 c_p - p_0 x c_p \tag{5}$$

$$\frac{dc_e}{dt} = t_1 - t_2 c_e - t_3 x c_e + t_3 x c_p \tag{6}$$

subject to initial conditions:

$$x(0) > 0,\ y(0) > 0,\ z(0) > 0,\ p(0) = 0,\ q(0) > 0.$$

3. Boundedness of Model

In this section, we derive upper bounds for prey, predator populations, and toxicant concentrations. Using comparison techniques and integral estimates, we demonstrate that the solutions of the system remain finite for all time. These results ensure that the model accurately reflects ecological dynamics and remains mathematically well-posed. The following theorem presents our findings formally.

Theorem 1. *The set* $\Omega = \{(x, y, z, c_p, c_e) \in R^5_+ : x(t) \leq 1, prx(t) + bry(t) + cpz(t) \leq m_1, t_3 c_p(t) + p_0 c_e(t) \leq m_2\}$, *where* $m_1 = \frac{2pr}{\phi_1}$ *and* $\phi_1 = \min\{1, q, s\}$, $m_2 = \frac{p_0 t_1}{\phi_2}$ *and* $\phi_2 = \min\{p_1, t_2\}$.

Proof. Let us consider

$$w_1(t) = prx(t) + bry(t) + cpz(t).$$

By differentiating both the sides, we get,

$$\frac{dw_1}{dt} = pr\frac{dx}{dt} + br\frac{dy}{dt} + cp\frac{dz}{dt},$$

from eqs. (2) to (4), obtained

$$\frac{dw_1}{dt} + \phi_1 w_1 \leq 2prx,$$

where $\phi_1 = \min\{1, q, s\}$ & then by the comparison theorem, $t \to \infty$, $w_1 \leq \frac{2pr}{\phi_1}$ and hence,

$$prx(t) + bry(t) + cpz(t) \leq m_1,$$

where $m_1 = \dfrac{2pr}{\phi_1}$. Now we will consider

$$w_2(t) = t_3 c_p + p_0 c_e.$$

By differentiating both the sides, we get,

$$\frac{dw_2}{dt} = t_3 \frac{dc_p}{dt} + p_0 \frac{dc_e}{dt},$$

from eqs. (5) and (6), we get,

$$\frac{dw_2}{dt} + \phi_2 w_2 \leq p_0 t_1,$$

where $\phi_2 = min\{p_1, t_2\}$& then by the comparison theorem, $t \to \infty$, $w_2 \leq \frac{p_0 t_1}{\phi_2}$ and hence,

$$t_3 c_p + p_0 c_e \leq m_2,$$

where $m_2 = \frac{p_0 t_1}{\phi_2}$.

Hence the solution of system is bounded in the region Ω. The boundedness of solutions confirms that the populations and toxicant concentrations remain within realistic limits, ensuring that the model does not predict ecological collapse or unbounded growth. □

4. Existence of Equilibria

Equilibrium points play a crucial role in understanding the long-term behavior of ecological systems. These points represent states where the population densities and toxicant concentrations remain constant over time. For our model, we have identified five equilibrium points, each corresponding to different ecological scenarios:

1. **Trivial Equilibrium:** $\tilde{E_1}(0, 0, 0, 0, \tilde{c_e})$ – Represents the extinction of all species.
2. **Prey-Only Equilibrium:** $\dot{E_2}(\dot{x}, 0, 0, \dot{c_p}, \dot{c_e})$ – Indicates a scenario where only the prey population survives.
3. **Prey and First Predator Coexistence:** $\ddot{E_3}(\ddot{x}, \ddot{y}, 0, \ddot{c_p}, \ddot{c_e})$ – Represents the coexistence of prey and the first predator while the second predator is absent.
4. **Prey and Second Predator Coexistence:** $\bar{E_4}(\bar{x}, 0, \bar{z}, \bar{c_p}, \bar{c_e})$ – Describes a scenario where the prey and the second predator coexist, but the intermediate predator is absent.
5. **Full Coexistence Equilibrium:** $E_5(x, y, z, c_p, c_e)$ – Represents a stable state where all species coexist.

The existence of these equilibria is analyzed through algebraic conditions derived from the system equations. In the following subsections, we establish the necessary conditions for each equilibrium to exist and discuss their biological significance.

4.1. *Existence of* $\tilde{E_1}(0, 0, 0, 0, \tilde{c_e})$

From eq. (6), we obtain,

$$\tilde{c_e} = \frac{t_1}{t_2} > 0.$$

Remark 1. The equilibrium concentration $\tilde{c_e} = \frac{t_1}{t_2}$ indicates that the environmental toxicant level is solely determined by the balance between its external input and removal rate. This implies that even in the absence of biological activity, the environment retains a persistent level of contamination.

4.2. *Existence of* $\dot{E_2}(\dot{x}, 0, 0, \dot{c_p}, \dot{c_e})$

From eq. (2), we get,

$$\dot{c_p} = \frac{(1 - \dot{x})}{g}.$$

with $\dot{c_p} > 0$ if $\dot{x} < 1$.

Remark 2. The equilibrium concentration of the toxicant within the organism is given by $\dot{c_p} = \frac{(1-\dot{x})}{g}$, which depends on the prey population size $(\dot{x})$ and the toxicant uptake factor (g). This expression indicates that as the prey population increases $(\dot{x} \to 1)$, the internal toxicant concentration decreases. Biologically, this suggests that a higher prey density dilutes the per capita toxicant burden, possibly due to a lower relative intake per individual or a reduced exposure effect. Conversely, if the prey population is low $(\dot{x} \to 0)$, the toxicant concentration within individuals rises, highlighting the vulnerability of small populations to toxicant accumulation.

Then, by solving equations eqs. (5) and (6), we obtain

$$\dot{c_e} = \frac{t_1 p_0 g - p_1 t_3 (1 - \dot{x})}{p_0 t_2 g}.$$

$\dot{c_e} > 0$, if $t_1 p_0 g > p_1 t_3 (1 - \dot{x})$. Furthermore, from eq. (5), the following polynomial equation is obtained

$$(p_1 t_3 + p_0 t_2)\dot{x}^2 + (p_0(t_1 g - t_2) - p_1(t_3 - t_2))\dot{x} - p_1 t_2 = 0.$$

This gives one positive root always.

4.3. *Existence of* $\ddot{E_3}(\ddot{x}, \ddot{y}, 0, \ddot{c_p}, \ddot{c_e})$

From eq. (3), we get,

$$\ddot{x} = \frac{q}{p - aq},$$

$\ddot{x} > 0$ if $p > aq$.

Remark 3. Biologically, this result signifies that the predator's conversion efficiency (p) must be sufficiently large relative to the product of its mortality rate (q) and the prey's regulatory effect (a) for a stable coexistence. If the predator's efficiency is too low $(p \leq aq)$, it cannot sustain itself, leading to possible collapse of the predator-prey interaction.

From eq. (2), we get,

$$\ddot{c_p} = \frac{(1 - \ddot{x})(1 + a\ddot{x}) - b\ddot{y}}{g(1 + a\ddot{x})},$$

where $\ddot{c_p} > 0$ if $(1-\ddot{x})(1+a\ddot{x}) > b\ddot{y}$ or $\ddot{y} < \frac{p(p-(a+1)q)}{b(p-aq)^2}$. Next, from eqs. (5) and (6), we obtained,

$$\ddot{c_e} = \frac{p_0t_1g(1+a\ddot{x}) + p_1t_3b\ddot{y} - p_1t_3(1-\ddot{x})(1+a\ddot{x})}{g(1+a\ddot{x})p_0t_2},$$

where $\ddot{c_e} > 0$, if $p_0t_1g(1+a\ddot{x}) + p_1t_3b\ddot{y} > p_1t_3(1-\ddot{x})(1+a\ddot{x})$. Lastly, from eq. (5), we have,

$$\ddot{y} = \frac{(1+a\ddot{x})((1-\ddot{x})(t_2(p_1+p_0\ddot{x}) + p_1t_3\ddot{x}) - p_0t_1g\ddot{x})}{p_1t_3b\ddot{x} + t_2b(p_1+p_0\ddot{x})},$$

$\ddot{y} > 0$, if satisfied $(1-\ddot{x})(t_2(p_1+p_0\ddot{x}) + p_1t_3\ddot{x}) > p_0t_1g\ddot{x}$.

4.4. Existence of $\bar{E_4}(\bar{x}, 0, \bar{z}, \bar{c_p}, \bar{c_e})$

From eq. (4), we get,

$$\bar{x} = \frac{s}{r-as},$$

with $\bar{x} > 0$ if $r > as$.

> **Remark 4.** Biologically, this result indicates that the prey population can sustain itself at equilibrium only if the predation pressure is not excessively high relative to the predator's natural death rate. If $r \leq as$, the prey population may decline to extinction, destabilizing the ecosystem.

From eq. (2), we get,

$$\bar{c_p} = \frac{r(r-(1+a)s) - (r-as)^2c\bar{z}}{rg(r-as)},$$

$\bar{c_p} > 0$ if $(1-\bar{x})(1+a\bar{x}) > c\bar{z}$. Then, from eqs. (5) and (6), we obtained,

$$\bar{c_e} = \frac{t_1p_0g(1+a\bar{x}) - p_1t_3(1-\bar{x})(1+a\bar{x}) + p_1t_3c\bar{z}}{p_0t_2g(1+a\bar{x})},$$

$$\bar{z} = \frac{(1+a\bar{x})((1-\bar{x})(t_2(p_1+p_0\bar{x}) + p_1t_3\bar{x}) - p_0t_1\bar{x})}{p_1t_3c\bar{x} + t_2c(p_1+p_0\bar{x})},$$

with $\bar{z} > 0$, if $(1-\bar{x})(t_2(p_1+p_0\bar{x}) + p_1t_3\bar{x}) > p_0t_1\bar{x}$.

4.5. Existence of $E_5(x, y, z, c_0, c_e)$

From eqs. (2) to (6), we obtained

$$\begin{aligned}
z &= \frac{x(p-aq)-q}{q},\\
y &= \frac{(r-as)x-s}{s},\\
c_p &= \frac{(1-x)(1+ax+z)(1+ax+y) - by(1+ax+y)}{g(1+ax+z)(1+ax+y)}\\
&\quad - \frac{cz(1+ax+z)}{g(1+ax+z)(1+ax+y)}\\
&= h_3(x),\\
c_e &= \frac{p_0t_1 - p_1t_3h_3(x)}{p_0t_2} = h_4(x),\\
x &= \frac{p_1h_3(x)}{p_0(h_4(x)-h_3(x))} = h_5(x).
\end{aligned}$$

$z,\ y,\ c_p,\ c_e,\ x > 0$, if each satisfied $x(p-aq) > q$, $(r-as)x > s$, $(1-x)(1+ax+z)(1+ax+y) > by(1+ax+y)+cz(1+ax+z)$, $p_0t_1 > p_1t_3h_3(x)$, $h_3(x) < h_4(x)$.

5. Local Stability Analysis of Equilibria

This section examines the stability of equilibrium points by evaluating the Jacobian matrix. Stability is determined by the eigenvalues. We analyze the characteristic equation and discuss the biological implications of stability conditions. The Jacobian matrix is given by:

$$J = \begin{bmatrix} \mathcal{A}_{11} & \mathcal{A}_{12} & \mathcal{A}_{13} & \mathcal{A}_{14} & 0 \\ \mathcal{A}_{21} & \mathcal{A}_{22} & \mathcal{A}_{23} & 0 & 0 \\ \mathcal{A}_{31} & \mathcal{A}_{32} & \mathcal{A}_{33} & 0 & 0 \\ \mathcal{A}_{41} & 0 & 0 & \mathcal{A}_{44} & \mathcal{A}_{45} \\ \mathcal{A}_{51} & 0 & 0 & \mathcal{A}_{54} & \mathcal{A}_{55} \end{bmatrix},$$

$$\begin{aligned}
\mathcal{A}_{11} &= 1-2x-gc_p - \frac{by(1+z)}{(1+ax+z)^2} - \frac{cz(1+y)}{(1+ax+y)^2},\\
\mathcal{A}_{12} &= \frac{-bx}{1+ax+z} + \frac{cxz}{(1+ax+y)^2},\\
\mathcal{A}_{13} &= \frac{bxy}{(1+ax+z)^2} - \frac{cx}{(1+ax+y)},\\
\mathcal{A}_{14} &= -gx, \qquad \mathcal{A}_{21} = \frac{py(1+z)}{(1+ax+z)^2},\\
\mathcal{A}_{22} &= \frac{px}{1+ax+z} - q, \qquad \mathcal{A}_{23} = \frac{-pxy}{(1+ax+z)^2},\\
\mathcal{A}_{31} &= \frac{rz(1+y)}{(1+ax+y)^2}, \qquad \mathcal{A}_{32} = \frac{-rxz}{(1+ax+y)^2},\\
\mathcal{A}_{33} &= \frac{rx}{(1+ax+y)} - s, \quad \mathcal{A}_{41} = p_0(c_e-c_p),\\
\mathcal{A}_{44} &= -(p_1+p_0x), \qquad \mathcal{A}_{45} = p_0x,\\
\mathcal{A}_{51} &= t_3(c_p-c_e), \qquad \mathcal{A}_{54} = t_3x,\\
\mathcal{A}_{55} &= -(t_2+t_3x).
\end{aligned}$$

To determine the eigenvalues, we solve the characteristic equation:

$$\det(J-\lambda I) = 0.$$

The eigenvalues determine the local stability of equilibrium points. If all the eigenvalues have negative real parts, the equilibrium is asymptotically stable. If at least one eigenvalue has a positive real part, then the equilibrium will be unstable.

5.1. Local stability of equilibrium $\tilde{E_1}(0, 0, 0, 0, \tilde{c_e})$

The local stability of the equilibrium point $\tilde{E_1}(0, 0, 0, 0, \tilde{c_e})$ by examining the Jacobian matrix J_1. The Jacobian matrix is given by:

$$J_1 = \begin{bmatrix} 1 & 0 & 0 & 0 & 0 \\ 0 & -q & 0 & 0 & 0 \\ 0 & 0 & -s & 0 & 0 \\ \frac{p_0t_1}{t_2} & 0 & 0 & -p_1 & 0 \\ \frac{-t_1t_3}{t_2} & 0 & 0 & 0 & -t_2 \end{bmatrix}. \tag{7}$$

The stability of $\tilde{E_1}$ is determined by analyzing the eigenvalues of J_1, which are:

$$\lambda_1 = 1,\ \lambda_2 = -q,\ \lambda_3 = -s,\ \lambda_4 = -p_1,\ \lambda_5 = -t_2.$$

Since one of the eigenvalue, $\lambda_1 = 1$, is positive, the equilibrium point $\tilde{E_1}$ is unstable.

5.2. *Local stability of equilibrium* $\dot{E}_2(\dot{x}, 0, 0, \dot{c_p}, \dot{c_e})$

Remark 5. The condition $\left(N < \frac{b_2}{a_1 b_1 - b_2}\right)$ implies that for the predator (P_1) to persist, the prey population must remain below a specific threshold. This threshold is determined by the balance between the natural death rate of (P_1) and its ability to convert consumed prey into its own population growth. If the prey population exceeds this limit, (P_1) may not sustain itself, potentially leading to its decline.

Remark 6. Similarly, the condition $\dot{E}_2$ $\left(N < \frac{c_2}{c_1 a_2 - c_2}\right)$ suggests that the second predator, (P_2), also requires the prey population to remain below a certain level for its stability. This threshold is influenced by the natural mortality rate of (P_2) and its predation efficiency. If the prey population surpasses this limit, (P_2) may struggle to survive, leading to possible extinction or reduced population levels.

We analyze the local stability of the equilibrium point $\dot{E}_2(\dot{x}, 0, 0, \dot{c_p}, \dot{c_e})$ by examining the Jacobian matrix J_2, which is given by:

$$J_2 = \begin{bmatrix} A_{11} & A_{12} & A_{13} & A_{14} & 0 \\ 0 & A_{22} & 0 & 0 & 0 \\ 0 & 0 & A_{33} & 0 & 0 \\ A_{41} & 0 & 0 & A_{44} & A_{45} \\ A_{51} & 0 & 0 & A_{54} & A_{55} \end{bmatrix},$$

$$\begin{aligned} A_{11} &= 1 - 2\dot{x} - g\dot{c_p}, & A_{12} &= \frac{-b\dot{x}}{1 + a\dot{x}}, \\ A_{13} &= \frac{-c\dot{x}}{(1 + a\dot{x})}, & A_{14} &= -g\dot{x}, \\ A_{22} &= \frac{p\dot{x}}{1 + a\dot{x}} - q, & A_{33} &= \frac{r\dot{x}}{(1 + a\dot{x})} - s, \\ A_{41} &= p_0(\dot{c_e} - \dot{c_p}), & A_{44} &= -(p_1 + p_0\dot{x}), \\ A_{45} &= p_0\dot{x}, & A_{51} &= -t_3(\dot{c_e} - \dot{c_p}), \\ A_{54} &= t_3\dot{x}, & A_{55} &= -(t_2 + t_3\dot{x}) \end{aligned} \tag{8}$$

To determine the stability of $\dot{E}_2$, we compute the eigenvalues of J_2. Out of five eigenvalues two of the eigenvalues are:

$$\lambda_1 = \frac{p\dot{x}}{1 + a\dot{x}} - q, \ \lambda_2 = \frac{r\dot{x}}{1 + a\dot{x}} - s.$$

These eigenvalues are negative if the following conditions hold:

$$\lambda_1 < 0, \text{ if } \frac{p\dot{x}}{1 + a\dot{x}} < q, \ \lambda_2 < 0, \text{ if } \frac{r\dot{x}}{1 + a\dot{x}} < s.$$

The remaining three eigenvalues are obtained from the characteristic polynomial:

$$\lambda^3 + T_1\lambda^2 + T_2\lambda + T_3 = 0.$$

The coefficients are given by:

$$\begin{aligned} T_1 &= (p_1 + p_0\dot{x}) - (1 - 2\dot{x} - g\dot{c_p}) + (t_2 + t_3\dot{x}), \\ T_2 &= p_0 g\dot{x}(\dot{c_e} - \dot{c_p}) - p_0 t_3\dot{x}^2 + (p_1 + p_0\dot{x})(t_2 + t_3\dot{x}) - (1 - 2\dot{x} \\ &\quad - g\dot{c_p})(p_1 + p_0\dot{x} + t_2 + t_3\dot{x}), \\ T_3 &= -(1 - 2\dot{x} - g\dot{c_p})(p_1(t_2 + t_3\dot{x}) + p_0 t_2\dot{x}) + p_0 g\dot{x} t_2(\dot{c_e} - \dot{c_p}). \end{aligned}$$

The equilibrium $\dot{E}_2$ is locally asymptotically stable if $T_1 > 0, T_2 > 0, T_3 > 0$ and $T_1 T_2 > T_3$ hold.

5.3. *Local stability of equilibrium* $\ddot{E}_3(\ddot{x}, \ddot{y}, 0, \ddot{c_p}, \ddot{c_e})$

To analyze the local stability of the equilibrium $\ddot{E}_3$, we consider the Jacobian matrix J_3:

$$J_3 = \begin{bmatrix} B_{11} & B_{12} & B_{13} & B_{14} & 0 \\ B_{21} & B_{22} & B_{23} & 0 & 0 \\ 0 & 0 & B_{33} & 0 & 0 \\ B_{41} & 0 & 0 & B_{44} & B_{45} \\ B_{51} & 0 & 0 & B_{54} & B_{55} \end{bmatrix},$$

$$\begin{aligned} B_{11} &= 1 - 2\ddot{x} - g\ddot{c_p} - \frac{b\ddot{y}}{(1 + a\ddot{x})^2}, & B_{12} &= \frac{-b\ddot{x}}{1 + a\ddot{x}}, \\ B_{13} &= \frac{b\ddot{x}\ddot{y}}{(1 + a\ddot{x})^2} - \frac{c\ddot{x}}{(1 + a\ddot{x} + \ddot{y})}, & B_{14} &= -g\ddot{x}, \\ B_{21} &= \frac{p\ddot{y}}{(1 + a\ddot{x})^2}, & B_{22} &= \frac{p\ddot{x}}{1 + a\ddot{x}} - q, \\ B_{23} &= \frac{-p\ddot{x}\ddot{y}}{(1 + a\ddot{x})^2}, & B_{33} &= \frac{r\ddot{x}}{(1 + a\ddot{x} + \ddot{y})} - s, \\ B_{41} &= p_0(\ddot{c_e} - \ddot{c_p}), & B_{44} &= -(p_1 + p_0\ddot{x}), \\ B_{45} &= p_0\ddot{x}, & B_{51} &= -t_3(\ddot{c_e} - \ddot{c_p}), \\ B_{54} &= t_3\ddot{x}, & B_{55} &= -(t_2 + t_3\ddot{x}). \end{aligned}$$

Out of five eigenvalues the one eigenvalue of the Jacobian matrix J_3 is:

$$\lambda_1 = \frac{r\ddot{x}}{1 + a\ddot{x} + \ddot{y}} - s.$$

This eigenvalue is negative if the following condition hold:

$$\lambda_1 < 0, \text{ if } \frac{r\ddot{x}}{1 + a\ddot{x} + \ddot{y}} < s.$$

The remaining four eigenvalues are determined from the characteristic equation:

$$\lambda^4 + R_1\lambda^3 + R_2\lambda^2 + R_3\lambda + R_4 = 0.$$

The coefficients are given by:

$$\begin{aligned} R_1 &= (t_2 + t_3\ddot{x}) + (p_1 + p_0\ddot{x}) - \left(1 - 2\ddot{x} - g\ddot{c_p} - \frac{b\ddot{y}}{(1 + a\ddot{x})^2}\right. \\ &\quad \left. + \frac{p\ddot{x}}{1 + a\ddot{x}} - q\right), \\ R_2 &= -(t_2 + t_3\ddot{x} + p_1 + p_0\ddot{x})\left(1 - 2\ddot{x} - g\ddot{c_p} - \frac{b\ddot{y}}{(1 + a\ddot{x})^2}\right. \\ &\quad \left. + \frac{p\ddot{x}}{1 + a\ddot{x}} - q\right) + p_0 t_3\ddot{x}^2 + (t_2 + t_3\ddot{x})(p_1 + p_0\ddot{x}) \\ &\quad + p_0 g\ddot{x}(\ddot{c_e} - \ddot{c_p}) + \frac{bp\ddot{x}\ddot{y}}{(1 + a\ddot{x})^3}, \\ R_3 &= -(p_0 t_3\ddot{x}^2 + (t_2 + t_3\ddot{x})(p_1 + p_0\ddot{x}))\left(1 - 2\ddot{x} - g\ddot{c_p}\right. \\ &\quad \left. - \frac{b\ddot{y}}{(1 + a\ddot{x})^2} + \frac{p\ddot{x}}{1 + a\ddot{x}} - q\right) + (p_1 + p_0\ddot{x} + t_2 \\ &\quad + t_3\ddot{x})\left(1 - 2\ddot{x} - g\ddot{c_p} - \frac{b\ddot{y}}{(1 + a\ddot{x})^2}\right)\left(\frac{p\ddot{x}}{1 + a\ddot{x}} - q\right), \end{aligned}$$

$$R_4 = (p_0t_3\ddot{x}^2 + (t_2 + t_3\ddot{x})(p_1 + p_0\ddot{x}))\Big(1 - 2\ddot{x} - g\ddot{c_p} - \frac{b\ddot{y}}{(1+a\ddot{x})^2}\Big)\Big(\frac{p\ddot{x}}{1+a\ddot{x}} - q\Big) - p_0g\ddot{x}(\ddot{c_e} - \ddot{c_p})\Big(\frac{p\ddot{x}}{1+a\ddot{x}} - q\Big)(t_2 + 2t_3\ddot{x}).$$

The equilibrium point $\ddot{E_3}$ is locally assymptotically slable if $R_1 > 0, R_2 > 0, R_3 > 0, R_4 > 0, R_1R_2 > R_3$ and $R_1R_2R_3 > (R_3^2 + R_1^2 + R_4)$ hold.

5.4. Local stability of equilibrium $\bar{E_4}(\bar{x}, 0, \bar{z}, \bar{c_p}, \bar{c_e})$

To analyze the local stability of the equilibrium $\bar{E_4}$, we consider the Jacobian matrix J_4:

$$J_4 = \begin{bmatrix} C_{11} & C_{12} & C_{13} & C_{14} & 0 \\ 0 & C_{22} & 0 & 0 & 0 \\ C_{31} & C_{32} & C_{33} & 0 & 0 \\ C_{41} & 0 & 0 & C_{44} & C_{45} \\ C_{51} & 0 & 0 & C_{54} & C_{55} \end{bmatrix},$$

$$C_{11} = 1 - 2\bar{x} - g\bar{c_p} - \frac{-c\bar{z}}{(1+a\bar{x})^2}, \; C_{13} = -\frac{c\bar{x}}{(1+a\bar{x})},$$
$$C_{12} = \frac{-b\bar{x}}{1+a\bar{x}+\bar{z}} + \frac{c\bar{x}\bar{z}}{(1+a\bar{x})^2}, \quad C_{14} = -g\bar{x},$$
$$C_{22} = \frac{p\bar{x}}{1+a\bar{x}+\bar{z}} - q, \; C_{31} = \frac{r\bar{z}}{(1+a\bar{x})^2},$$
$$C_{32} = \frac{-r\bar{x}\bar{z}}{(1+a\bar{x})^2}, \qquad C_{33} = \frac{r\bar{x}}{(1+a\bar{x})} - s,$$
$$C_{41} = p_0(\bar{c_e} - \bar{c_p}), \qquad C_{44} = -(p_1 + p_0\bar{x}),$$
$$C_{45} = p_0\bar{x}, \qquad C_{51} = -t_3(\bar{c_e} - \bar{c_p}),$$
$$C_{54} = t_3\bar{x}, \qquad C_{55} = -(t_2 + t_3\bar{x}).$$

Out of five eigenvalues the one eigenvalue of the Jacobian matrix J_4 is given by

$$\lambda_1 = \frac{p\bar{x}}{1+a\bar{x}+\bar{z}} - q.$$

This eigenvalue is negative if the following condition hold:

$$\lambda_1 < 0, \text{ if } \frac{p\bar{x}}{1+a\bar{x}+\bar{z}} < q.$$

The remaining four eigenvalues are determined from the characteristic equation:

$$\lambda^4 + S_1\lambda^3 + S_2\lambda^2 + S_3\lambda + S_4 = 0.$$

The coefficients are given by:

$$S_1 = (t_2 + t_3\bar{x}) + (p_1 + p_0\bar{x}) - \Big(1 - 2\bar{x} - g\bar{c_p} - \frac{c\bar{z}}{(1+a\bar{x})^2} - \frac{r\bar{x}}{1+a\bar{x}} - s\Big),$$

$$S_2 = p_0t_3\bar{x}^2 + (p_1 + p_0\bar{x})(t_2 + t_3\bar{x}) + p_0g\bar{x}(\bar{c_e} - \bar{c_p}) - \Big(1 - 2\bar{x} - g\bar{c_p} - \frac{c\bar{z}}{(1+a\bar{x})^2} - \frac{r\bar{x}}{1+a\bar{x}} - s\Big)(t_2 + t_3\bar{x} + p_1 + p_0\bar{x}) - \Big(1 - 2\bar{x} - g\bar{c_p} - \frac{c\bar{z}}{(1+a\bar{x})^2}\Big)\Big(\frac{r\bar{x}}{1+a\bar{x}} + s\Big) + \frac{cr\bar{x}\bar{z}}{(1+a\bar{x})^3},$$

$$S_3 = -(p_0t_3\bar{x}^2 + (p_1 + p_0\bar{x})(t_2 + t_3\bar{x}))\Big(1 - 2\bar{x} - g\bar{c_p} - \frac{c\bar{z}}{(1+a\bar{x})^2} - \frac{r\bar{x}}{1+a\bar{x}} - s\Big) - (p_1 + p_0\bar{x} + t_2 + t_3\bar{x})\Big(1 - 2\bar{x} - g\bar{c_p} - \frac{c\bar{z}}{(1+a\bar{x})^2}\Big)\Big(\frac{r\bar{x}}{1+a\bar{x}} + s\Big) + (p_1 + p_0\bar{x} + t_2 + t_3\bar{x})\frac{cr\bar{x}\bar{z}}{(1+a\bar{x})^3} + p_0g\bar{x}(\bar{c_e} - \bar{c_p})\Big(t_2 + 2t_3\bar{x} + \Big(\frac{r\bar{x}}{1+a\bar{x}} + s\Big)\Big),$$

$$S_4 = -\Big(1 - 2\bar{x} - g\bar{c_p} - \frac{c\bar{z}}{(1+a\bar{x})^2}\Big)\Big(\frac{r\bar{x}}{1+a\bar{x}} + s\Big)(p_0t_3\bar{x}^2 + (p_1 + p_0\bar{x})(t_2 + t_3\bar{x})) + p_0g\bar{x}\Big(\frac{r\bar{x}}{1+a\bar{x}} + s\Big)(\bar{c_e} - \bar{c_p})(t_2 + 2t_3\bar{x}) + \frac{cr\bar{x}\bar{z}}{(1+a\bar{x})^3}(p_0t_3\bar{x} + (p_1 + p_0\bar{x})(t_2 + t_3\bar{x})).$$

The equilibrium point E_4 is locally assymptotically slable if $S_1 > 0, S_2 > 0, S_3 > 0, S_4 > 0, S_1S_2 > S_3$ and $S_1S_2S_3 > (S_3^2 + S_1^2S_4)$ hold.

5.5. Local stability of equilibrium $E_5(x, y, z, c_p, c_e)$

To analyze the local stability of the equilibrium E_5, we consider the Jacobian matrix J_5:

$$J_5 = \begin{bmatrix} A_{11} & \frac{-bx}{\alpha} + \frac{cxz}{\beta^2} & \frac{bxy}{\alpha^2} - \frac{cx}{\beta} & -gx & 0 \\ \frac{p\phi}{\alpha^2} & \frac{px}{\alpha} - q & \frac{-pxy}{\alpha^2} & 0 & 0 \\ \frac{r\psi}{\beta^2} & \frac{rxz}{\beta^2} & \frac{rx}{\beta} - s & 0 & 0 \\ p_0\gamma & 0 & 0 & -\xi & p_0x \\ -t_3\gamma & 0 & 0 & t_3x & -\omega \end{bmatrix},$$

$$A_{11} = 1 - 2x - gc_p - \frac{b\phi}{\alpha^2} - \frac{c\psi}{\beta^2}, \; \alpha = (1 + ax + z),$$
$$\beta = (1 + ax + y), \qquad \gamma = (c_e - c_p),$$
$$\xi = (p_1 + p_0x), \qquad \omega = (t_2 + t_3x),$$
$$\phi = y(1 + z), \qquad \psi = z(1 + y).$$

The eigenvalues are determined from the characteristic equation:

$$\lambda^5 + P_1\lambda^4 + P_2\lambda^3 + P_3\lambda^2 + P_4\lambda + P_5 = 0.$$

The coefficients are given by:

$$P_1 = \omega + \xi - A_{11} - \Big(\frac{px}{\alpha} - q + \frac{rx}{\beta} - s\Big),$$

$$P_2 = -p_0x(t_3x + \gamma g) + \xi\omega - A_{11}(\omega + \xi) + \Big(\frac{px}{\alpha} - q\Big)\Big(\frac{rx}{\beta} - s\Big) - \Big(\frac{px}{\alpha} - q + \frac{rx}{\beta} - s\Big)(\omega + \xi - A_{11}) - \frac{prx^2yz}{\alpha^2\beta^2} - \frac{p\phi}{\alpha^2}\Big(\frac{-bx}{\alpha} + \frac{cxz}{\beta^2}\Big) - \frac{r\psi}{\beta^2}\Big(\frac{bxy}{\alpha^2} + \frac{cx}{\beta}\Big),$$

$$P_3 = [(t_3x + \gamma g)p_0x + (\omega + \xi)A_{11} - \xi\omega]\Big(\frac{px}{\alpha} - q + \frac{rx}{\beta} - s\Big) + (\omega + \xi - A_{11})\Big(\frac{px}{\alpha} - q\Big)\Big(\frac{rx}{\beta} - s\Big) - \frac{p}{\alpha^2}\Big[(\omega + \xi)\phi - \Big(\frac{rx}{\beta} - s\Big)\phi - \frac{rxy\psi}{\beta^2}\Big]\Big(\frac{-bx}{\alpha} + \frac{cxz}{\beta^2}\Big) - \frac{r}{\beta^2}\Big[(\omega^2 + \xi)\psi - \frac{pxz}{\alpha^2}\phi - \Big(\frac{px}{\alpha} - q\Big)\psi\Big]\Big(\frac{bxy}{\alpha^2} - \frac{cx}{\beta}\Big) - (\omega + \xi$$

$$- A_{11})\frac{prx^2yz}{\alpha^2\beta^2} + p_0\gamma gx(t_3x-\omega) + A_{11}(p_0t_3x^2-\xi\omega),$$

$$P_4 = [(\xi\omega - p_0t_3x^2)A_{11} + p_0\gamma gx(\omega - t_3x)]\left(\frac{px}{\alpha} - q + \frac{rx}{\beta} - s\right)\left(\frac{px}{\alpha} - q + \frac{rx}{\beta} - s\right) + [\xi\omega - A_{11}(\omega+\xi) - p_0x(t_3x+\gamma g)]\left(\frac{px}{\alpha} - q\right)\left(\frac{rx}{\beta} - s\right) + \frac{p}{\alpha^2}\left[(p_0t_3x^2 - \xi\omega)\phi + (\omega+\xi)\phi\left(\frac{rx}{\beta} - s\right) + (\omega+\xi)\frac{rxy\psi}{\beta^2}\right]\left(\frac{-bx}{\alpha} - \frac{cxz}{\beta^2}\right) + \frac{r}{\beta^2}\left[(p_0t_3x^2 - \xi\omega)\psi + (\omega+\xi)\psi\left(\frac{px}{\alpha} - q\right) + (\omega+\xi)\frac{pxz\phi}{\alpha^2}\right]\left(\frac{bxy}{\alpha^2} - \frac{cx}{\beta}\right) + \left((t_3x+\gamma g)p_0x + (\omega+\xi)A_{11} - \xi\omega\right)\frac{prx^2yz}{\alpha^2\beta^2},$$

$$P_5 = [(t_3x-\omega)p_0\gamma gx + (p_0t_3x^2 - \xi\omega)A_{11}]\left(\frac{px}{\alpha} - q\right)\left(\frac{rx}{\beta} - s\right) + \frac{p}{\alpha^2}(\xi\omega - p_0t_3x^2)\left[\phi\left(\frac{rx}{\beta} - s\right) + \frac{rxy\psi}{\beta^2}\right]\left(\frac{-bx}{\alpha} + \frac{cxz}{\beta^2}\right) + \frac{r}{\beta^2}(\xi\omega - p_0t_3x^2)\left[\psi\left(\frac{px}{\alpha} - q\right) + \frac{pxz\phi}{\alpha^2}\right]\left(\frac{bxy}{\alpha^2} - \frac{cx}{\beta}\right) + [(\omega - t_3x^2)p_0\gamma g + (\xi\omega - p_0t_3x^2)A_{11}].$$

The equilibrium point E_5 is locally assymptotically slable if $P_1 > 0, P_2 > 0, P_3 > 0, P_4 > 0, P_5 > 0, P_1P_2 > P_3, P_1P_2P_3 > (P_3^2 + P_1^2P_4)$ and $(P_3P_4 - P_2P_5)(P_1P_2 - P_3) > (P_1P_4 - P_5)^2$ hold.

6. Global Stability

In this section, we establish the global stability of the equilibrium point $E_5(x, y, z, c_p, c_e)$ within the bounded region Ω. By constructing a suitable Lyapunov function and applying LaSalle's Invariance Principle [26], we derive sufficient conditions under which the system converges globally to this equilibrium. The following theorem presents the necessary conditions for global asymptotic stability.

Theorem 2. *In the region Ω, if the following conditions hold:*

$$a\left(\frac{b\overline{y}}{\sigma_1} - \frac{c\overline{z}}{\sigma_2}\right) < 1, \tag{9}$$

$$p_1 + p_0x > 0, \tag{10}$$

$$t_2 + t_3x > 0, \tag{11}$$

$$\left(1 - \frac{ab\overline{y}}{\sigma_1} - \frac{ac\overline{z}}{\sigma_2}\right)(t_2 + t_3x) > A_4t_3^2(\overline{c_e} - \overline{c_p})^2, \tag{12}$$

where

$$\sigma_1 = (1 + ax + z)(1 + a\overline{x} + \overline{z}),$$
$$\sigma_2 = (1 + ax + y)(1 + a\overline{x} + \overline{y}),$$
$$A_1 = \frac{b\sigma_2(1 + a\overline{x} + \overline{z} - \sigma_1c\overline{z})}{p(1+\overline{z})\sigma_2} > 0,$$
$$A_2 = \frac{c\sigma_1(1 + a\overline{x} + \overline{y} - \sigma_2b\overline{y})}{r(1+\overline{y})\sigma_1} > 0,$$
$$A_3 = \frac{g}{p_0(\overline{c_e} - \overline{c_p})},$$
$$A_4 = \frac{-g}{t_3(\overline{c_e} - \overline{c_p})},$$

then $E_5(x, y, z, c_p, c_e)$ will be globally asymptotically stable in the region Ω.

Proof. Let us consider the following Lyapunov function:

$$V_{11} = \left[x - \overline{x} - \overline{x}\log\left(\frac{x}{\overline{x}}\right)\right] + A_1\left[y - \overline{y} - \overline{y}\log\left(\frac{y}{\overline{y}}\right)\right] + A_2\left[z - \overline{z} - \overline{z}\log\left(\frac{z}{\overline{z}}\right)\right] + \frac{A_3}{2}(c_p - \overline{c_p})^2 + \frac{A_4}{2}(c_e - \overline{c_e})^2.$$

Differentiating both side with respect to t, we get,

$$\frac{dV_{11}}{dt} = \left(\frac{x-\overline{x}}{x}\right)\frac{dx}{dt} + A_1\left(\frac{y-\overline{y}}{y}\right)\frac{dy}{dt} + A_2\left(\frac{z-\overline{z}}{z}\right)\frac{dz}{dt} + A_3(c_p - \overline{c_p})\frac{dc_p}{dt} + A_4(c_e - \overline{c_e})\frac{dc_e}{dt}.$$

From eqs. (2) to (6), we get,

$$\frac{dV_{11}}{dt} = -(x-\overline{x})^2 - g(x-\overline{x})(c_p - \overline{c_p}) - \frac{b}{\sigma_1}(x-\overline{x})(y-\overline{y}) - \frac{ab}{\sigma_1}\overline{x}(x-\overline{x})(y-\overline{y}) + \frac{ab}{\sigma_1}\overline{y}(x-\overline{x})^2 - \frac{b}{\sigma_1}\overline{z}(x-\overline{x})(y-\overline{y}) + \frac{b}{\sigma_1}\overline{y}(x-\overline{x})(z-\overline{z}) - \frac{c}{\sigma_2}(x-\overline{x})(z-\overline{z}) - \frac{ac}{\sigma_2}\overline{x}(x-\overline{x})(z-\overline{z}) + \frac{ac}{\sigma_2}\overline{z}(x-\overline{x})^2 - \frac{c}{\sigma_2}\overline{y}(x-\overline{x})(z-\overline{z}) + \frac{c}{\sigma_2}\overline{z}(y-\overline{y}),$$

where

$$\sigma_1 = (1 + ax + z)(1 + a\overline{x} + \overline{z}),\ \sigma_2 = (1 + ax + y)(1 + a\overline{x} + \overline{y}),$$

and choosing

$$A_1 = \frac{b\sigma_2(1 + a\overline{x} + \overline{z} - \sigma_1c\overline{z})}{p(1+\overline{z})\sigma_2} > 0,$$
$$A_2 = \frac{c\sigma_1(1 + a\overline{x} + \overline{y} - \sigma_2b\overline{y})}{r(1+\overline{y})\sigma_1} > 0,$$
$$A_3 = \frac{g}{p_0(\overline{c_e} - \overline{c_p})},$$
$$A_4 = \frac{-g}{t_3(\overline{c_e} - \overline{c_p})}.$$

Now, $\frac{dV_{11}}{dt}$ can be written as

$$\frac{dV_{11}}{dt} \le -\left[\frac{b_{11}}{2}(x-\overline{x})^2 + b_{15}(x-\overline{x})(c_e - \overline{c_e}) + \frac{b_{55}}{2}(c_e - \overline{c_e})^2 + b_{44}(c_p - \overline{c_p})^2\right],$$

where,

$$b_{11} = 1 - \frac{ab\overline{y}}{\sigma_1} - \frac{ac\overline{z}}{\sigma_2},$$
$$b_{44} = A_3p_1 + A_3p_0x,$$
$$b_{55} = A_4t_2 + A_4t_3x,$$
$$b_{15} = A_4t_3\overline{c_e} - A_4t_3\overline{c_p}.$$

By the Sylvester's criteria, we get that $\frac{dV_{11}}{dt}$ will be negative function with the inequalities:

$$b_{11} > 0, \tag{13}$$
$$b_{44} > 0, \tag{14}$$
$$b_{55} > 0, \tag{15}$$
$$b_{11}b_{55} > b_{15}^2. \tag{16}$$

We note that the inequalities, eq. (9) $\Rightarrow$ eq. (13), eq. (10) $\Rightarrow$ eq. (14), eq. (11) $\Rightarrow$ eq. (15) and eq. (12) $\Rightarrow$ eq. (16). Hence V_{11} of E_5 in Ω. Proved theorem. □

From the above analysis, it follows that under the given conditions, the equilibrium point E_5 is globally asymptotically stable. The constructed Lyapunov function demonstrates that the system's trajectories eventually settle at E_5, ensuring long-term persistence and stability of the interacting populations. Thus, the system exhibits a globally stable dynamical behaviour, reinforcing the robustness of equilibrium under perturbations.

7. Numerical Simulation

In this section, we perform a comprehensive numerical analysis to validate the analytical results obtained for the system's equilibrium points. We present stability graphs for equilibria E_2, E_3, E_4 and E_5, illustrating their dynamical behavior under different initial conditions. Additionally, we analyze bifurcation patterns to explore critical parameter thresholds that lead to qualitative changes in system dynamics. Sensitivity analysis is also conducted to examine the impact of key parameters on system stability and behavior. These numerical simulations provide deeper insights into the model's real-world applicability and reinforce the analytical findings.

7.1. *Stability analysis*

The stability of equilibrium points is a fundamental aspect of dynamical systems, as it determines whether small perturbations around an equilibrium will decay or grow over time. In this section, we analyze the stability of equilibrium points, E_2, E_3, E_4 and E_5 by computing their corresponding eigenvalues and interpreting their significance in the context of the system's dynamics. Furthermore, we verify that these results satisfy the conditions of local stability obtained in our calculations.

Example 1. For the given parameter values, which are assumed to ensure biologically realistic dynamics and to facilitate the study of system behavior under various conditions:

$$\begin{array}{llllllllll} a_0 = 10, & b_0 = 1.5, & c_0 = 1.8, & a_1 = 1.5, \\ r_1 = 1, & a_2 = 1.2, & r_2 = 0.8, & b_1 = 0.5, \\ b_2 = 2.5, & c_1 = 0.5, & c_2 = 1.5, & d_1 = 2.8, \\ e_1 = 0.5, & e_2 = 1.5, & q_0 = 2.5, & e_3 = 1.2, \end{array}$$

the system attains an equilibrium point at:

$$E_2(4.1549,\ 0.0000,\ 0.0000,\ 2.0929,\ 1.2114).$$

The stability of this equilibrium is confirmed by the computed eigenvalues:

$$\lambda = (-18.6802,\ -6.3711,\ -0.7467,\ -1.8955,\ -1.0164),$$

all of which have negative real parts, indicating that E_2 is locally asymptotically stable. The corresponding stability graph is presented in Figure 1, which visually confirms the equilibrium's stability.

Example 2. For the given parameter values, which are assumed to ensure biologically realistic dynamics and to facilitate the study of system behavior under various conditions:

$$\begin{array}{llllllllll} a_0 = 10, & b_0 = 1.2, & c_0 = 1.5, & a_1 = 1.5, \\ r_1 = 1, & a_2 = 1.2, & r_2 = 0.8, & b_1 = 2.1, \\ b_2 = 2.63, & c_1 = 0.5, & c_2 = 1.5, & d_1 = 2.8, \\ e_1 = 0.5, & e_2 = 1.5, & q_0 = 2.5, & e_3 = 1.2, \end{array}$$

the system attains an equilibrium point at:

$$E_3(5.0670,\ 3.0543,\ 0.0000,\ 2.1086,\ 1.2053).$$

The stability of this equilibrium is confirmed by the computed eigenvalues:

$$\lambda = (-22.6574,\ -5.4725,\ -0.0586,\ -0.7469,\ -1.1428),$$

all of which have negative real parts, indicating that E_3 is locally asymptotically stable. The corresponding stability graph is presented in Figure 2, which visually confirms the equilibrium's stability.

Example 3. For the given parameter values, which are assumed to ensure biologically realistic dynamics and to facilitate the study of system behavior under various conditions:

$$\begin{array}{llllllllll} a_0 = 10, & b_0 = 1.2, & c_0 = 1.5, & a_1 = 1.5, \\ r_1 = 1, & a_2 = 1.2, & r_2 = 0.8, & b_1 = 2.1, \\ b_2 = 2.63, & c_1 = 1.5, & c_2 = 1.51, & d_1 = 2.8, \\ e_1 = 0.5, & e_2 = 1.5, & q_0 = 2.5, & e_3 = 1.2, \end{array}$$

the system attains an equilibrium point at:

$$E_4(5.4024,\ 0.0000,\ 1.8505,\ 2.1149,\ 1.2016).$$

The stability of this equilibrium is confirmed by the computed eigenvalues:

$$\lambda = (-24.1057,\ -6.2587,\ -0.0042,\ -0.7451,\ -0.5680),$$

all of which have negative real parts, indicating that E_4 is locally asymptotically stable. The corresponding stability graph is presented in Figure 3, which visually confirms the equilibrium's stability.

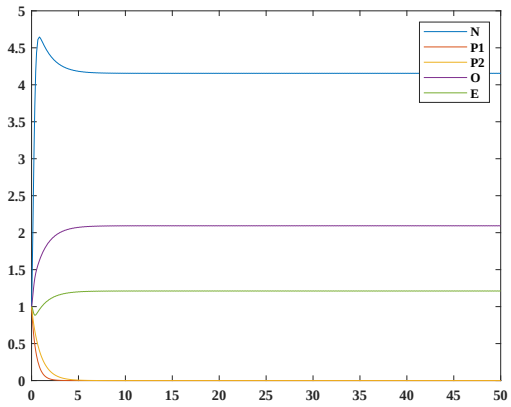

Figure 1. Stable dynamics of the system at equilibrium $E_2(N, 0, 0, O, E)$, where species P_1 and P_2 go extinct while other variables stabilize.

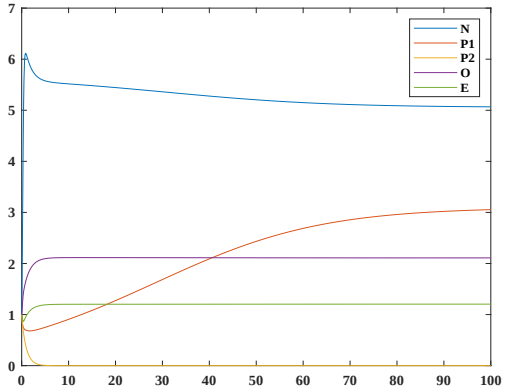

Figure 2. Stable dynamics of the system at equilibrium $E_3(N, P_1, 0, O, E)$, where species P_2 goes extinct while P_1 persists along with other variables.

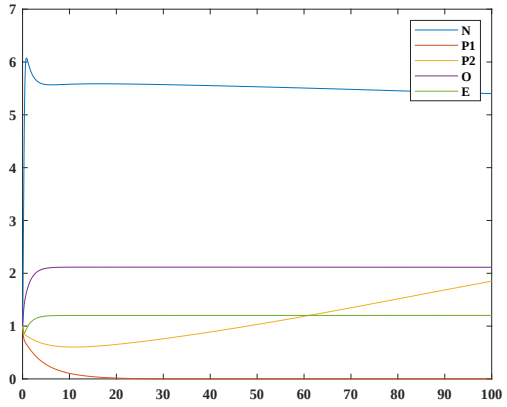

Figure 3. Stable dynamics of the system at equilibrium $E_4(N, 0, P_2, O, E)$, where species P_1 goes extinct while P_2 persists along with other variables.

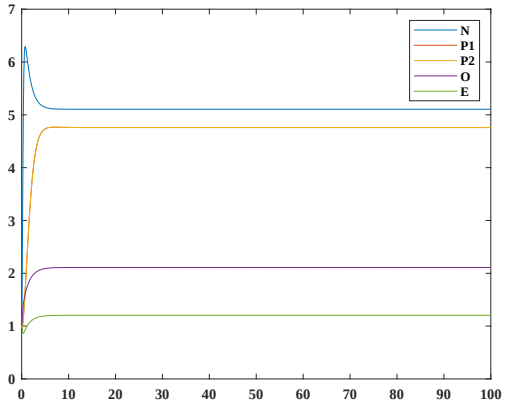

Figure 4. Stable dynamics of the system at equilibrium $E_5(N, P_1, P_2, O, E)$, where both species P_1 and P_2 coexist with other variables stabilizing.

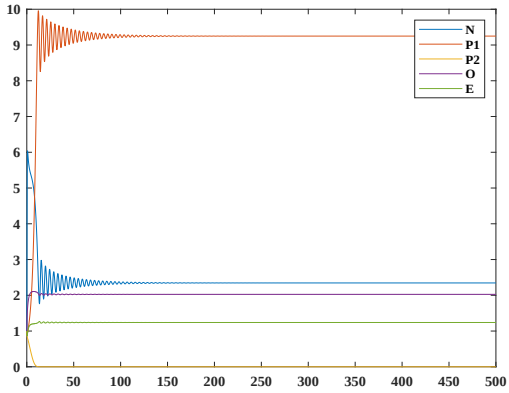

Figure 5. Stable dynamics of the system at equilibrium $E_3(N, P_1, 0, O, E)$, where species P_2 is absent and other variables stabilizing after initial oscillations.

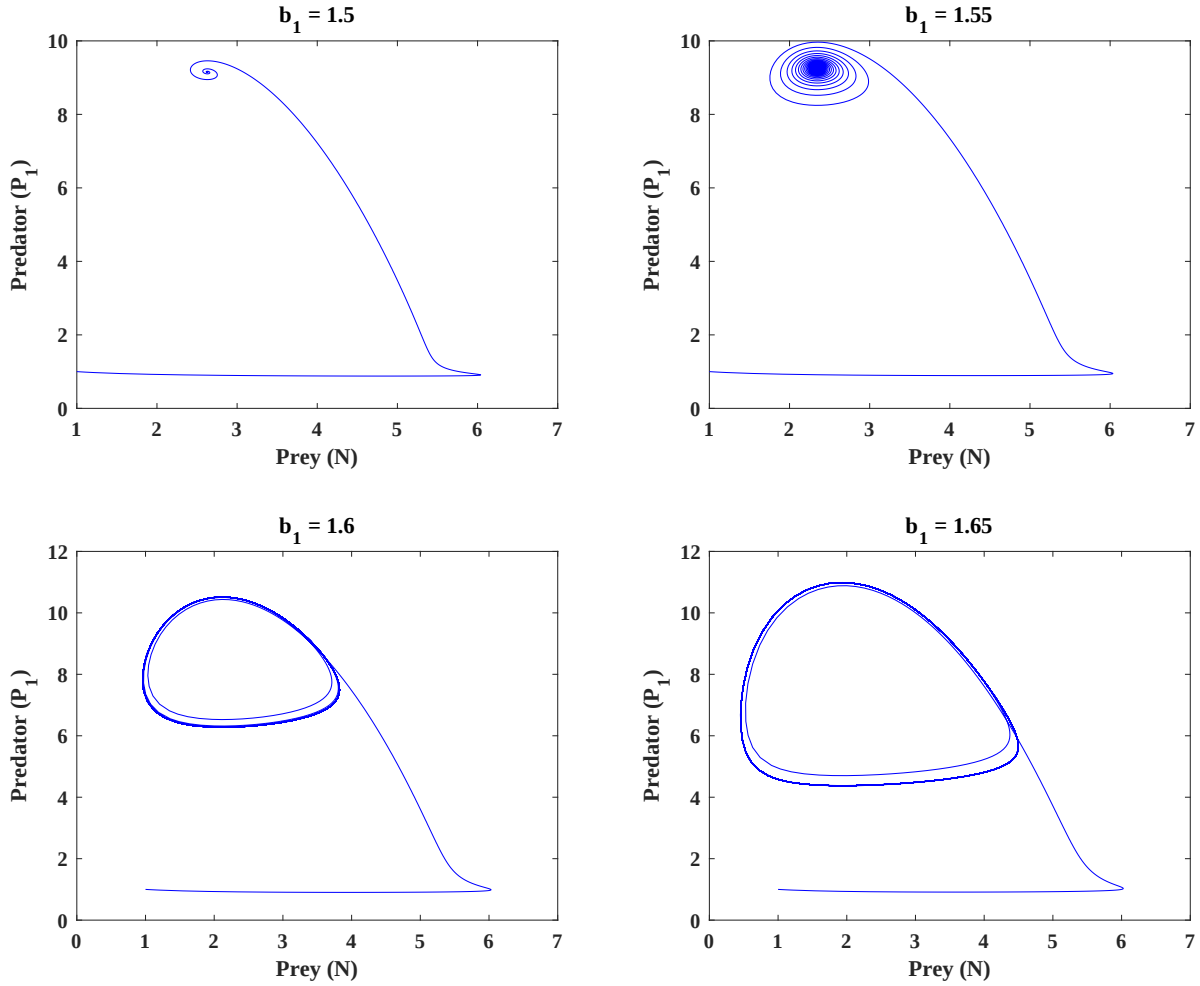

Figure 6. Phase trajectories of the system for different values of b_1. As b_1 increases from 1.5 to 1.65, the system transitions from a stable equilibrium to a stable limit cycle, indicating a Hopf bifurcation.

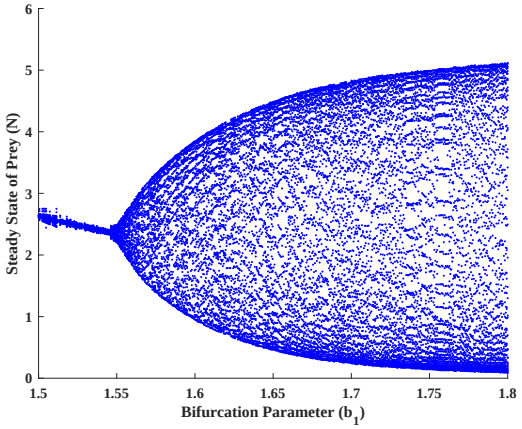

Figure 7. Bifurcation diagram for prey population N with respect to b_1.

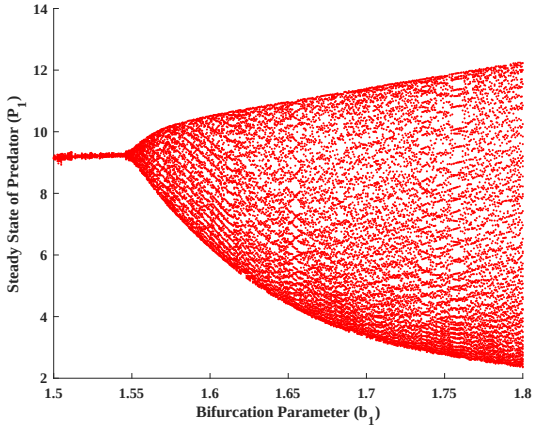

Figure 8. Bifurcation diagram for predator population P_1 with respect to b_1.

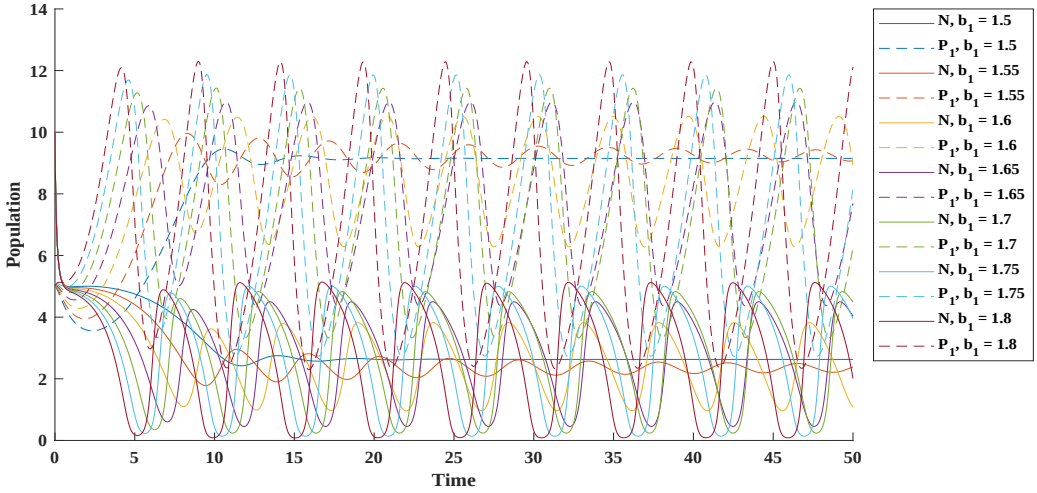

Figure 9. Time series dynamics of N and P_1 for varying b_1 values.

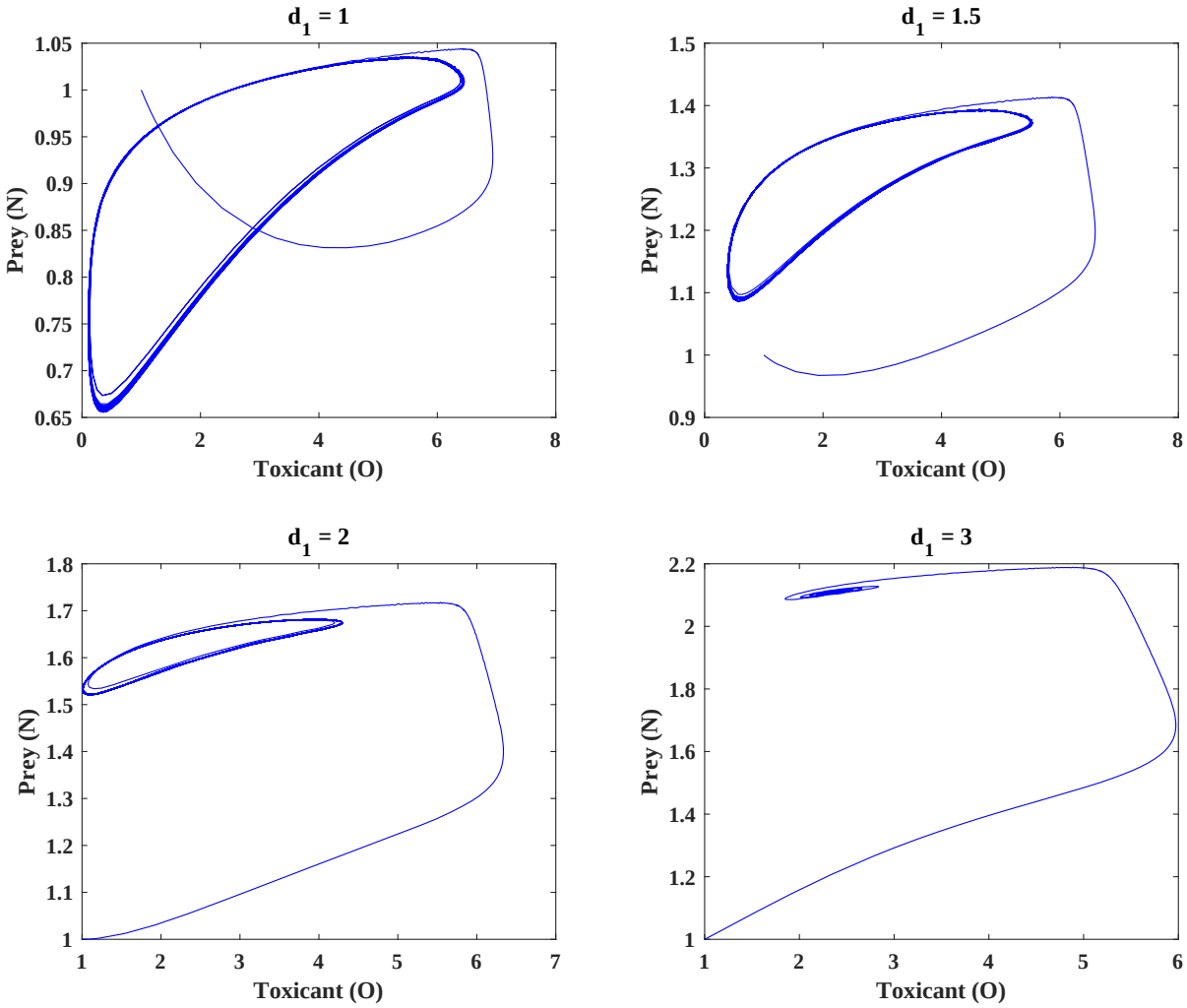

Figure 10. Phase trajectories of prey N and toxicant O for different values of d_1, showing system dynamics and stability variations.

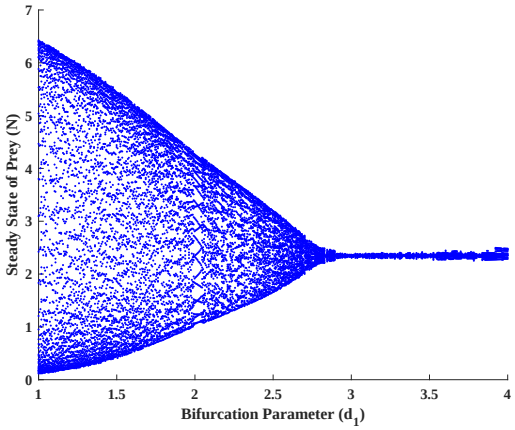

Figure 11. Bifurcation diagram showing the steady-state behavior of prey N as the bifurcation parameter d_1 varies.

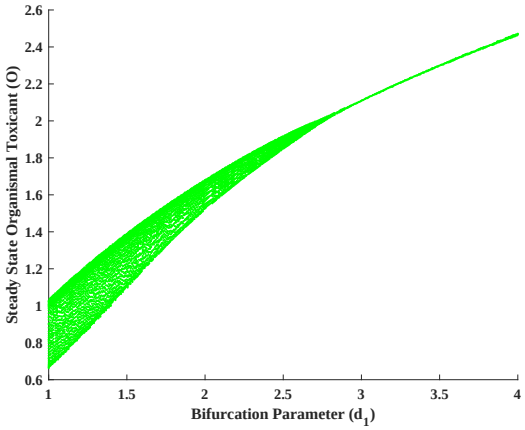

Figure 12. Bifurcation diagram depicting the steady-state levels of toxicant O with respect to the bifurcation parameter d_1.

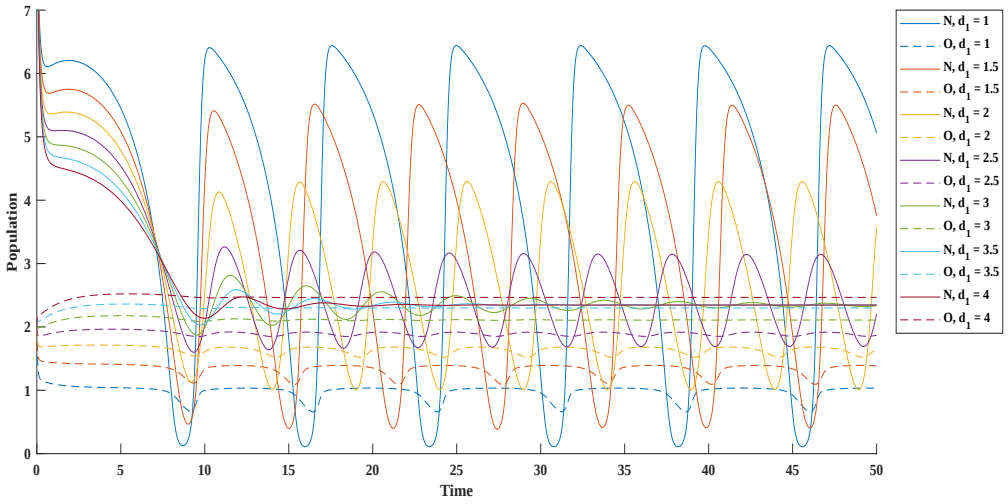

Figure 13. Time series dynamics of prey N and toxicant O populations for different values of the bifurcation parameter d_1.

Example 4. For the given parameter values, which are assumed to ensure biologically realistic dynamics and to facilitate the study of system behavior under various conditions:

$$\begin{array}{llllll} a_0 = 10.5, & b_0 = 1.2, & c_0 = 1.5, \\ a_1 = 1.5, & r_1 = 1.2, & a_2 = 1.5, \\ r_2 = 1.2, & b_1 = 2.515, & b_2 = 1.63, \\ c_1 = 2.515, & c_2 = 1.63, & d_1 = 2.8, \\ e_1 = 0.5, & e_2 = 1.5, & q_0 = 2.5, \\ e_3 = 1.2, \end{array}$$

the system attains an equilibrium point at:

$$E_5(5.1057,\ 4.7591,\ 4.7591,\ 2.1103,\ 1.2039).$$

The stability of this equilibrium is confirmed by the computed eigenvalues:

$$\lambda = (-22.8260,\ -5.5664,\ -0.9141,\ -0.7411,\ -0.7878),$$

all of which have negative real parts, indicating that E_5 is locally asymptotically stable. The corresponding stability graph is presented in Figure 4, which visually confirms the equilibrium's stability.

Example 5. For the given parameter values, which are assumed to ensure biologically realistic dynamics and to facilitate the study of system behavior under various conditions:

$$\begin{array}{llllll} a_0 = 10, & b_0 = 1.2, & c_0 = 1.5, \\ a_1 = 1.5, & r_1 = 1, & a_2 = 1.2, \\ r_2 = 0.8, & b_1 = 1.55, & b_2 = 1.63, \\ c_1 = 1.5, & c_2 = 1.51, & d_1 = 2.8, \\ e_1 = 0.5, & e_2 = 1.5, & q_0 = 2.5, \\ e_3 = 1.2, \end{array}$$

the system attains an equilibrium point at:

$$E_3(2.3455,\ 9.2493,\ 0.0000,\ 2.0261,\ 1.2388).$$

The stability of this equilibrium is confirmed by the computed eigenvalues:

$$\lambda = (-10.9235,\ -0.7138,\ -1.1171,\ -0.0281 \pm 1.4490i),$$

all of which have negative real parts, indicating that E_3 is locally asymptotically stable. The corresponding stability graph is presented in Figure 5, which visually confirms the equilibrium's stability.

7.2. *Bifurcation analysis*

Bifurcation refers to a qualitative change in the long-term behavior of a dynamical system as a parameter is varied [28, 29]. In particular, a Hopf bifurcation occurs when a stable equilibrium loses stability, giving rise to a periodic solution (limit cycle). This transition is significant in ecological modeling as it helps identify conditions under which populations shift from stable states to oscillatory or chaotic dynamics. To analyze the effect of parameter variation, we study the system's behavior for different values of b_1 of Example 5. The phase portraits shown in Figure 6 illustrate the trajectories of the system for different values of b_1, specifically for $b_1 = 1.5, 1.55, 1.6, 1.65$. At $b_1 = 1.5$, the trajectory converges to the equilibrium, confirming its stability. However, as b_1 increases to 1.55, a small periodic orbit appears, indicating the onset of a Hopf bifurcation. Further increments in b_1 to 1.6 and 1.65 lead to more pronounced oscillatory behavior, signifying a transition to complex dynamics. To understand the system's long-term behavior, bifurcation diagrams are presented in Figures 7 and 8. These diagrams depict the steady states of the prey N and predator P_1 populations as functions of b_1. For lower values of b_1, the equilibrium remains stable. As b_1 increases and crosses a threshold around 1.55, a Hopf bifurcation occurs, leading to the emergence of oscillations. With further increments in b_1, period-doubling bifurcations appear, eventually resulting in chaotic dynamics. To complement this analysis, the time series behavior of the prey and predator populations is shown in Figure 9. For $b_1 = 1.5$, the populations stabilize at equilibrium. However, as b_1 increases, oscillations emerge and become more pronounced. Beyond $b_1 = 1.65$, irregular fluctuations suggest a transition to chaotic behavior. This extended analysis highlights the crucial role of b_1 in influencing the system's stability and dynamics. The results confirm that the system undergoes a Hopf bifurcation, followed by period-doubling bifurcations leading to chaos. These findings provide deeper insights into the system's complex behavior under parameter variations and emphasize the significance of bifurcation analysis in ecological modeling. For the given parameter values, as in Example 5, we analyze the effect of varying d_1 on the system's dynamics while keeping all other parameters constant. The phase portraits Figure 10 illustrate the trajectories of the system for different values of d_1. At lower values of d_1 , such as $d_1 = 1$, the prey population N and organismal toxicant O exhibit sustained oscillations, forming closed trajectories that indicate the presence of a limit cycle and instability in the system. As d_1 increases to 1.5 and 2, the oscillatory behavior persists but becomes more structured. However, at $d_1 = 3$, the oscillations diminish significantly, and the trajectory stabilizes, indicating a transition toward a steady-state equilibrium. This suggests that increasing d_1 enhances the stability of the system. To further understand the impact of d_1 , bifurcation diagrams Figures 11 and 12, depict the steady-state values of prey N and organismal toxicant O as functions of d_1. For lower values of d_1, the prey population undergoes complex oscillations, and bifurcations appear, signifying an unstable regime. As d_1 increases, the oscillations gradually reduce, leading to a stable equilibrium. Similarly, the toxicant concentration O fluctuates at smaller d_1 values but stabilizes at higher d_1, confirming that an increase in d_1 mitigates toxicant accumulation and supports a balanced prey population. The time series analysis Figure 13 provides additional insight into the system's long-term behavior. For smaller values of d_1, such as $d_1 = 1$ and $d_1 = 1.5$, the populations of prey N and toxicant O exhibit sustained oscillations, indicating periodic behavior. As d_1 increases, the amplitude of these oscillations decreases, suggesting a transition toward stability. At $d_1 = 3$, both prey and toxicant populations reach a steady-state equilibrium, reinforcing the conclusion that higher values of d_1 contribute to system stabilization. Overall, this analysis highlights the critical role of d_1 in influencing system stability. Initially, lower d_1 values lead to oscillatory and unstable dynamics, but as d_1 increases, the system undergoes a transition toward stability. This finding suggests that an appropriate increase in d_1 can help regulate toxicant accumulation and promote a stable ecological balance.

8. Conclusion

This study presents a comprehensive mathematical analysis of a prey-predator system with two competing predators, incorporating the Beddington–DeAngelis functional response and the effects of environmental toxicants. Analytical investigations established the boundedness of the system, ensuring biologically feasible solutions. Equilibrium points were determined, and their stability was analysed through eigenvalue computations, confirming that stability depends on key system parameters.

Numerical simulations validated the analytical findings by demonstrating the system's dynamic transitions under parameter variations. Phase trajectory analysis revealed that as b_1 increased, the system transitioned from a stable equilibrium to periodic oscillations and eventually to chaotic behaviour. This progression was further confirmed through bifurcation diagrams, which highlighted critical thresholds where stability was lost. Time-series simulations illustrated how fluctuations in predator-prey populations intensified with increasing b_1, reinforcing the presence of Hopf and period-doubling bifurcations.

Additionally, the role of the toxicant uptake rate d_1 was examined to assess its influence on system stability. The results revealed that for lower values of d_1 , oscillatory behaviour persisted due to reduced toxicant accumulation in prey, allowing predator populations to fluctuate. However, as d_1 increased, the intensified toxicant exposure led to reduced prey availability, ultimately stabilizing the system. Beyond a certain threshold, the system transitioned from periodic oscillations to a stable equilibrium, as excessive toxicant absorption suppressed prey and predator population growth. These findings highlight the dual

role of toxicants, while moderate toxicant uptake induces instability, excessive uptake can stabilize population dynamics.

From an ecological perspective, this study underscores the critical influence of toxicant absorption and interspecies competition on population stability. The results suggest that while increased toxicant levels may initially disrupt ecological balance, they can also impose a stabilizing effect by limiting population growth. Understanding these non-linear interactions is essential for ecological management, particularly in environments affected by pollution.

Overall, this study integrates analytical analysis and numerical simulations to provide a deeper understanding of the interplay between toxicants, predator-prey interactions, and bifurcation phenomena. The findings contribute to ecological modelling by emphasizing the importance of toxicant dynamics in shaping ecosystem stability and offer potential insights for environmental conservation and pollution control strategies.

In order to evaluate their effects on system stability and bifurcation dynamics, future studies can expand on this work by investigating different functional responses, such as ratio-dependent, sigmoidal, or other generic predator-prey interactions. In order to gain a better understanding of inter specific competition and cohabitation in multi-predator environments, the model can be extended to incorporate more than two competing predators. Prey refuge mechanisms, in which a portion of the prey population is shielded from predators, are another crucial avenue that can drastically change population dynamics and stability conditions. Can extend this model by incorporating fractional-order derivatives to capture memory effects in ecological interactions, as demonstrated by Manivel et al. [27] in disease modelling. These advancements could enhance ecological modelling and inform better conservation policies.

Author Contributions. **Makwana, K.**: Mathematical analysis, numerical simulations, software implementation, writing-original draft preparation, data visualization (graphs). **Babu A., R.**: Formulation of the mathematical model, conceptualization, methodology. **Jadon, B.P.S**: Supervision.

Acknowledgement. The authors sincerely thank the editors and reviewers for their valuable feedback, which has helped improve the manuscript. We also appreciate the insightful discussions and guidance from our colleagues and mentors during this work.

Funding. This research received no external funding.

Conflict of interest. The authors declare no conflict of interest.

Data availability. Not applicable.

References

[1] J. D. Murray, *"Mathematical Biology I: An Introduction,"* 3 Edition, Springer Nature, 2002. DOI:10.1007/b98868

[2] N. Zhang, Y. Kao, and B. Xie, "Impact of fear effect and prey refuge on a fractional order prey–predator system with Beddington–DeAngelis functional response," *Chaos*, vol. 32, pp. 1–17, 2022. DOI:10.1063/5.0082733

[3] Y. Shao and W. Kong, "A Predator–Prey Model with Beddington–DeAngelis Functional Response and Multiple Delays in Deterministic and Stochastic Environments," *Mathematics*, vol. 10, no. 18, p. 3378, 2022. DOI:10.3390/math10183378

[4] X. Y. Meng and J. G. Wang, "Analysis of a Delayed Diffusive Model with Beddington–DeAngelis Functional Response," *Int. J. Biomath.*, vol. 12, no. 4, p. 1950047, 2019. DOI:10.1142/s1793524519500475

[5] E. Rahmi *et al.*, "A Modified Leslie–Gower Model Incorporating Beddington–DeAngelis Functional Response, Double Allee Effect, and Memory Effect," *Fractal and Fractional*, vol. 5, no. 3, p. 84, 2021. DOI:10.3390/fractalfract5030084

[6] S. Yu and F. Chen, "Dynamic Behaviors of a Competitive System with Beddington-DeAngelis Functional Response," *Discrete Dynamics in Nature and Society*, vol. 2019, pp. 1–12, 2019. DOI:10.1155/2019/4592054

[7] R. Babu and P. Gayathri, "Mathematical Study of One Prey and Two Competing Predators Considering Beddington-DeAngelis Functional Response with Distributed Delay," *Hilbert Journal of Mathematical Analysis*, vol. 2, no. 1, pp. 1–19, 2023. DOI:10.62918/hjma.v2i1.14

[8] S. N. Majeed and R. K. Naji, "Dynamical Behavior of Two Predators-One Prey Ecological System with Refuge and Beddington–DeAngelis Functional Response," *Iraqi Journal of Science*, vol. 64, no. 12, pp. 6383-–6400, 2023. DOI:10.24996/ijs.2023.64.12.24

[9] Q. Zhou and F. Chen, "Dynamical Analysis of a Discrete Amensalism System with the Beddington–DeAngelis Functional Response and Allee Effect for the Unaffected Species," *Qual. Theory Dyn. Syst.*, vol. 22, no. 16, 2022. DOI:10.1007/s12346-022-00716-5

[10] H. I. Freedman and J. B. Shukla, "Models for the effect of toxicant in single-species and predator-prey systems," *Journal of mathematical biology*, vol. 30, no. 1, pp. 15–30, 1991. DOI:10.1007/BF00168004

[11] A. R. Babu, K. Yadav and B. P. S. Jadon, "The study of top predator interference on tri species with "food-limited" model under the toxicant environment: A mathematical implication," *Liberte Journal*, vol. 13, no. 1, pp. 20–35, 2025.

[12] B. K. Das, N. Santra, and G. Samanta, "Exploring dynamics of predator-prey interactions: fear, toxicity, carry over and environmental fluctuations," *Filomat*, vol. 38, no. 31, pp. 11061–11083, 2024. DOI:10.2298/FIL2431061D

[13] C. Liu *et al.*, "Bifurcation and Stability Analysis of a New Fractional-Order Prey–Predator Model with Fear Effects in Toxic Injections," *Mathematics*, vol. 11, no. 20, p. 4367, 2023. DOI:10.3390/math11204367

[14] O. P. Misra and A. R. Babu, "A model for the dynamical study of food-chain system considering interference of top predator in a polluted environment," *Journal of Mathematical Modeling*, vol. 3, no. 2, pp. 189–218, 2016.

[15] O. P. Misra and A. R. Babu, "Modelling the Effect of Toxicant on a Three Species Food-Chain System with Predator Harvesting," *International Journal of Applied and Computational Mathematics,* , vol. 3, no. 1, pp. 71–97, 2017. DOI:10.1007/s40819-017-0342-4

[16] O. P. Misra and A. R. Babu, "Modelling effect of toxicant in a three-species food-chain system incorporating delay in toxicant uptake process by prey," *Modeling Earth Systems and Environment*, vol. 2, no. 77, pp. 1–27, 2016. DOI:10.1007/s40808-016-0128-4

[17] J. Danane, M. Yavuz, and M. Yıldız, "Stochastic Modeling of Three-Species Prey–Predator Model Driven by Levy Jump with Mixed Holling-II and Beddington–DeAngelis Functional Responses," *Fractal and Fractional*, vol. 7, no. 10, p. 751, 2023. DOI:10.3390/fractalfract7100751

[18] S. Bosi and D. Desmarchelier, "Local bifurcations of three and four-dimensional systems: A tractable characterization with economic applications," *Mathematical Social Sciences*, vol. 97, pp. 38–50, 2019. DOI:10.1016/j.mathsocsci.2018.11.001

[19] N. Wang *et al.*, "Bifurcation Behavior Analysis in a Predator-Prey Model," *Discrete Dynamics in Nature and Society*, vol. 2016, no. 1, pp. 1–11, 2016. DOI:10.1155/2016/3565316

[20] R. P. Kaur *et al.*, "Chaos control of chaotic plankton dynamics in the presence of additional food, seasonality, and time delay," *Chaos, Solitons and Fractals*, vol. 153, p. 111521, 2021. DOI:10.1016/j.chaos.2021.111521

[21] H. S. Panigoro and E. Rahmi, "Computational dynamics of a Lotka-Volterra Model with additive Allee effect based on Atangana-Baleanu fractional derivative," *Jambura Journal of Biomathematics (JJBM)*, vol. 2, no. 2, pp. 96–103, 2021. DOI:10.34312/jjbm.v2i2.11886

[22] S. Bhatter *et al.*, "A new investigation on fractionalized modeling of human liver," *Scientific Reports*, vol. 14, no. 1, p. 1636, 2024. DOI:10.1038/s41598-024-51430-y

[23] S. Kumawat *et al.*, "Numerical modeling on age-based study of coronavirus transmission," *Applied Mathematics in Science and Engineering*, vol. 30, no. 1, pp. 609–634, 2022. DOI:10.1080/27690911.2022.2116435

[24] M. Meena *et al.*, "A novel fractionalized investigation of tuberculosis disease," *Applied Mathematics in Science and Engineering*, vol. 32, no. 1, 2024. DOI:10.1080/27690911.2024.2351229

[25] D. Mukherjee, "Impact of predator fear on two competing prey species," *Jambura Journal of Biomathematics (JJBM)*, vol. 2, no. 1, pp. 1–12, 2021. DOI:10.34312/jjbm.v2i1.9249

[26] Shyamsunder and S. D. Purohit, "A novel study of the impact of vaccination on pneumonia via fractional approach," *Partial Differential Equations in Applied Mathematics*, vol. 10, p. 100698, 2024. DOI:10.1016/j.padiff.2024.100698

[27] M. Manivel, A. Venkatesh, and S. Kumawat, "Numerical simulation for the co-infection of Monkeypox and HIV model using fractal-fractional operator," *Modeling Earth Systems and Environment*, vol. 11, no. 157, 2025. DOI:10.1007/s40808-025-02359-2

[28] D. Mukherjee, "Fear induced dynamics on Leslie-Gower predator-prey system with Holling-type IV functional response," *Jambura Journal of Biomathematics (JJBM)*, vol. 3, no. 2, pp. 49–57, 2022. DOI:10.34312/jjbm.v3i2.14348

[29] L. K. Beay and M. Saija, "Dynamics of a stage–structure Rosenzweig–MacArthur model with linear harvesting in prey and cannibalism in predator," *Jambura Journal of Biomathematics (JJBM)*, vol. 2, no. 1, pp. 42–50, 2021. DOI:10.34312/jjbm.v2i1.10470